



ELSEVIER

Marine and Petroleum Geology xx (0000) xxx–xxx

---



---

Marine and  
Petroleum Geology

---



---

[www.elsevier.com/locate/marpetgeo](http://www.elsevier.com/locate/marpetgeo)

# Hydrocarbon filling history from diagenetic evidence: Brent Group, UK North Sea

Mark Wilkinson<sup>a,\*</sup>, R. Stuart Haszeldine<sup>a</sup>, Robert M. Ellam<sup>b</sup>, Tony E. Fallick<sup>b</sup>

<sup>a</sup>*Department of Geology and Geophysics, Grant Institute, University of Edinburgh, West Mains Road, Edinburgh, Scotland EH9 3JW, UK*

<sup>b</sup>*Scottish Universities Environmental Research Centre, East Kilbride, Scotland G75 0QF, UK*

Received 30 January 2003; received in revised form 18 June 2003; accepted 29 July 2003

## Abstract

Reconstruction of the hydrocarbon filling history of a reservoir is important for prediction of field-scale porosity and permeability, and for the calibration of basin models. Published histories of the Brent Group show for only a single phase of hydrocarbon filling, which occurred after the diagenetic reactions had run their course. In contrast, diagenetic minerals preserve evidence of multiple episodes of hydrocarbon charging. In the Cormorant Field, UK North Sea, authigenic blocky kaolin shows a systematic change in oxygen isotopic composition with depth, and the trend displays a conspicuous shift at the Mid-Ness Shale, a regionally extensive permeability barrier. The isotopic data are most readily explained if kaolin recrystallisation (from earlier vermiform kaolin) was synchronous with hydrocarbon charging, with two hydrocarbon pools, one above and one below the Mid-Ness Shale. The filling history begins with a relatively early, slow, filling phase (45–70 °C; 80–50 Ma) that formed an oil column with the oil–water contact substantially below the present-day position. This first hydrocarbon subsequently leaked off, allowing renewed diagenetic activity, including the formation of quartz overgrowths with aqueous inclusions. Emplacement of the present-day hydrocarbon charge was the last event in the history of the reservoir (90–100 °C; 10–0 Ma). © 2003 Published by Elsevier Ltd.

*Keywords:* Kaolin; Diagenesis; Porosity; Reservoir quality

## 1. Introduction

The timing of oil charge into a trap is of interest to any geologist trying to gain a thorough understanding of an asset or prospect. However, the methods available are limited, and the results sometimes ambiguous because there are no direct methods of dating petroleum migration. Analysis of diagenetic minerals can provide an indirect estimate of the timing of reservoir filling: some reservoirs contain diagenetic illite that can be dated using the K–Ar system. It has been proposed that this illite grows at the time of oil filling (Hamilton, Kelley, & Fallick, 1989) though the physical or chemical mechanism remains obscure (Darby, Wilkinson, Fallick, & Haszeldine, 1997; Wilkinson & Haszeldine, 2002). In recent years, basin models have become increasingly popular as tools for the understanding of sedimentary basins and their hydro-geological systems, but these must be calibrated to field-specific measurements if their predictions

are to be reliable. For heat flow for example, data such as vitrinite-reflectance or spore colouration can provide the constraints required for meaningful modelling. And while a basin model will predict either the timing of oil migration or, at least, the time when the kitchen areas become mature, calibration data are more difficult to obtain. This paper examines diagenetic evidence for the timing and duration of hydrocarbon charge, providing a new method for the possible calibration of basin models into the geological past, and for the reconstruction of complex reservoir filling histories.

Many published oil-field descriptions and diagenetic histories (paragenetic sequences as they are termed) show only a single phase of oil emplacement, and this is nearly always the last diagenetic event. Examples for the Brent Group include Haszeldine, Brint, Fallick, Hamilton, and Brown (1992) and Osborne, Haszeldine, and Fallick (1994). However, it is entirely possible for a trap to have a more complex filling history, which may even involve emptying due to, for example, seal failure (Deighton, 1996) and subsequent refilling with hydrocarbon.

\* Corresponding author. Tel.: +44-131-650-5943; fax: +44-131-668-3184.

E-mail address: [m.wilkinson@glg.ed.ac.uk](mailto:m.wilkinson@glg.ed.ac.uk) (M. Wilkinson).

57  
58  
59  
60  
61  
62  
63  
64  
65  
66  
67  
68  
69  
70  
71  
72  
73  
74  
75  
76  
77  
78  
79  
80  
81  
82  
83  
84  
85  
86  
87  
88  
89  
90  
91  
92  
93  
94  
95  
96  
97  
98  
99  
100  
101  
102  
103  
104  
105  
106  
107  
108  
109  
110  
111  
112

113 It has been hypothesised that oil charging prevents  
 114 diagenesis within the oil-saturated portions of the reservoir,  
 115 or at least dramatically slows the rates of mineral reactions  
 116 (Bloch, Lander, & Bonnell, 2002; Worden, Smalley, &  
 117 Oxtoby, 1998). This has been demonstrated for individual  
 118 reservoirs, where careful measurement of cement volumes,  
 119 and modelling of thermal histories, enables the influence of  
 120 oil emplacement to be quantified (Deighton, 1996; Marc-  
 121 hand, Haszeldine, Smalley, Macaulay, & Fallick, 2001).  
 122 The influence of early hydrocarbon charging on reservoir  
 123 quality is still controversial (Marchand, Smalley, Haszel-  
 124 dine, & Fallick, 2002). The theoretical link between oil and  
 125 diagenesis is simple: the diagenetic reactions all take place  
 126 in the water phase within the rock, and chemical species  
 127 must diffuse through the water, and/or advect, from mineral  
 128 to mineral. In an oil-filled reservoir, the residual water has a  
 129 complex 3D shape with tortuous flow paths. This restricts  
 130 the movement of the chemical species (which cannot travel  
 131 through the oil), and hence slows the reactions. Even in a  
 132 water-wet reservoir (where the grain surfaces are covered in  
 133 a thin film of water), the pathways available for diffusion  
 134 between adjacent mineral grains are tortuous, so slowing  
 135 diffusion, and the effective water permeability can be very  
 136 low (Honarpour, Koederitz, & Harvey, 1986) so slowing  
 137 advection. Thus early oil charge can prevent the mineral  
 138 reactions that lead to chemical compaction, the growth of  
 139 mineral cements during burial that occlude porosity, and  
 140

169 the diagenetic dissolution of feldspar and other minerals  
 170 during deep burial that generate secondary porosity  
 171 (Wilkinson, Darby, Haszeldine, & Couples, 1997). Conse-  
 172 quently, early oil charge can preserve high porosities to  
 173 unusual depths of burial (Bloch et al., 2002; Heasley,  
 174 Worden, & Hendry, 2000).

175 In this study, diagenetic evidence is described from the  
 176 Cormorant Field of the East Shetland Basin of the Northern  
 177 North Sea (Fig. 1). From the sequence of clay minerals, and  
 178 isotopic ratios, we deduce that there was an early oil charge  
 179 which leaked off, and that subsequently the reservoir re-  
 180 filled with hydrocarbon. Previous work has inferred only a  
 181 single phase of oil filling, relatively late in the field history,  
 182 corresponding to peak oil generation (Taylor & Dietvorst,  
 183 1991). The Cormorant Field is an approximately north–  
 184 south oriented horst structure (Demyttenaere, Sluijk, &  
 185 Bentley, 1993), the petroleum geology of which is described  
 186 by Taylor and Dietvorst (1991). There are four major oil  
 187 pools, the largest of which is termed Cormorant IV. This is a  
 188 down-faulted anticline to the east of the main horst, with a  
 189 very complex faulted structure (Demyttenaere et al., 1993).  
 190 The Brent Group in Cormorant IV is juxtaposed with the  
 191 Permo-Triassic sediments of the main Cormorant structure,  
 192 locally called the Cormorant Group (Demyttenaere et al.,  
 193 1993). The reservoir within Cormorant IV is the Brent  
 194 Group, which has been well described in the literature as a  
 195 regressive–transgressive marginal marine-deltaic clastic  
 196

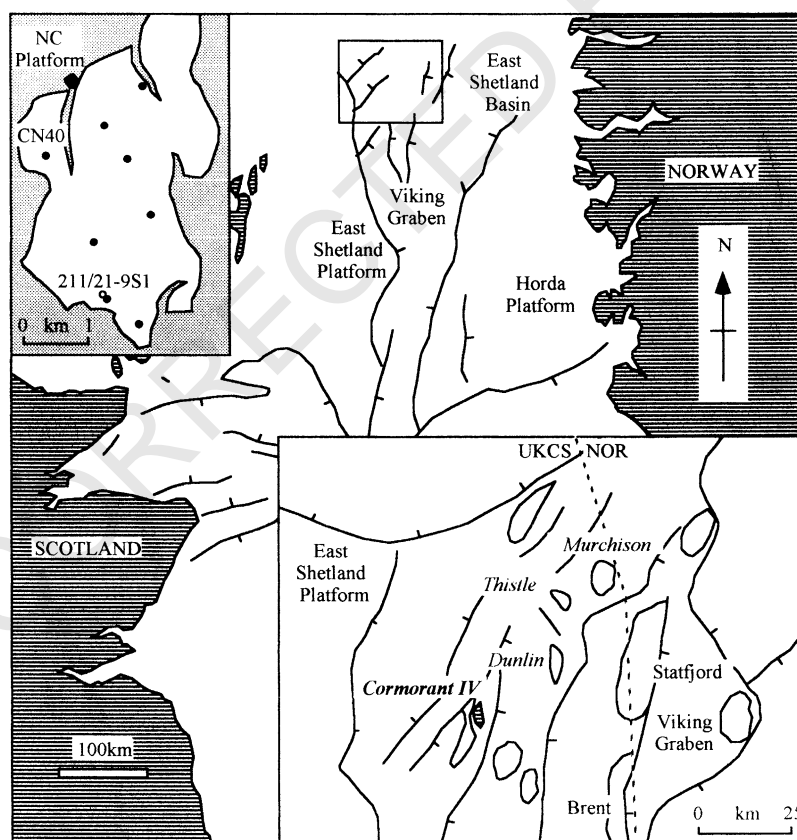


Fig. 1. Location map with inset map of the East Shetland Basin (lower right) and field plan showing the 8 wells sampled (upper left).

system (Morton, Haszeldine, Giles, & Brown, 1992). The dominant lithology is medium grained sandstone, with interbedded shales. Some of the shales are regionally extensive, such as the 4–6 m thick Mid-Ness shale that sub-divides the sequence into an upper and lower reservoir unit (Howe, 1992) and extends over 2100 km<sup>2</sup> (Richards, 1992). A total of eight wells were chosen for study, giving a wide geographic coverage over the field (Fig. 1). Previous published work on the diagenesis of the Cormorant Field is limited to Wilkinson, Haszeldine, Fallick, and Osborne (2000) that presented isotopic and petrographic data for siderite, and a number of papers concerning illite (Giles et al., 1992; Hamilton, Giles, & Ainsworth, 1992; Kantorowicz, 1990). The field is presently at its maximum depth of burial, and there is no evidence that the present-day temperature has ever been exceeded. This has been measured as the flowing bottom hole temperature of 97–105 °C (25 measurements). The oil–water contact is presently at ca. 2990–3000 m depth in well CN40.

## 2. Methods

Sandstone samples for study were collected from core. A total of 109 thin-sections were prepared (blue resin impregnated and stained for feldspars and carbonates) for petrographic examination, and chips of rock examined on an SEM. Sandstone composition was assessed using point-counting (200 counts per thin-section, performed by Badley-Ashton and Associates Ltd), using both our own thin-sections and those supplied by Shell UK (a further 120 samples). Polished thin-sections were prepared for CL and BS-SEM examination. The paragenetic sequence was established using standard optical petrography using thin-sections, and SEM examination of both polished thin-sections and rock chips. All sample depths are relative to the sea surface, and are measured perpendicular to this surface (true vertical depth).

For stable oxygen isotopic analysis of authigenic minerals, separates of kaolin and quartz overgrowth were prepared using settling and centrifugation techniques described by Brint (1989). Analytical conditions were described by Fallick, Macaulay, and Haszeldine (1993); analytical precision is  $\pm 0.2$  ( $1\sigma$ ). Data are presented in standard  $\delta$ -notation relative to the V-SMOW standard. Due to the small size of available samples from well CN40 (most were 2.5 cm diameter core plugs originally drilled for measurement of porosity and permeability), it was necessary to group the core plugs in order to obtain sufficient sample for analysis. This was done on a stratigraphic basis, hence all samples were made up of two or three plugs from only a single formation. Depth ranges are given in Table 2. A single water sample taken during a drill stem test (DST) was available from well 211/21-9S1 (Fig. 1), although the stratigraphic interval from which the porewater was obtained is unknown. Porewater oxygen isotope ratios

were measured by a modification of the carbon dioxide equilibration method (Epstein & Mayeda, 1953); the accuracy and precision ( $1\sigma$ ) are  $\pm 0.2\%$ . Hydrogen isotope ratios were made on hydrogen gas produced by reduction over Cr (Donnelly, Waldron, Tait, Dougans, & Bearhop, 2001); precision and accuracy ( $1\sigma$ ) are  $\pm 1\%$ .

Fluid inclusions were studied using double polished wafers 40–100  $\mu\text{m}$  thick, prepared so as to avoid unnecessary stress and temperatures exceeding 50 °C. Temperature of homogenisation ( $T_h$ ) was determined using a Reynolds gas-flow US Geological Survey-modified stage mounted on a Leitz Ortholux II microscope. Ultra-violet fluorescence was carried out on the same microscope. Analytical error is small ( $\pm 1$  °C) compared to the range of the results.

## 3. Results

A summary of sandstone compositions from point-counting is given in Table 1. The majority of the rocks are sub-arkoses according to the classification of Pettijohn, Potter, and Seiver (1973) (Fig. 2). Kaolin occurs in two crystal habits, as verms (Fig. 3a) and blocky crystals (Fig. 3c). The two crystal habits commonly occur together, with blocky crystals in the spaces within the verms (Fig. 3b). In this case, the platy sub-crystals within the verms have irregular margins suggestive of partial dissolution. We interpret the vermiform kaolin to be early in the paragenetic sequence (it occurs as a minor phase enclosed within some early concretions; Fig. 3d) and that it progressively dissolves while the blocky kaolin crystals grow within the spaces in the verms. The degree of recrystallisation of an individual verm is highly variable within a single sandstone sample, making it impossible to correlate the degree of recrystallisation to isotopic composition. The clays within the sandstones are generally stained by oil, which fluoresces yellow–white in UV light. Some of the secondary porosity

Table 1  
Summary of sandstone composition for well CN40 ( $n = 30$ )

	Mean value	2 Standard errors
Quartz	52.8	4.9
K–feldspar	7.6	1.1
Plagioclase	0.6	0.1
Rock fragments	2.2	0.6
Muscovite	3.5	1.6
Indeterminate clay	5.0	2.0
Kaolin	3.4	1.2
Fe–calcite	8.8	6.3
Siderite	1.2	0.9
Quartz overgrowths	1.7	0.9
Feldspar overgrowths	0.1	0.1
Pyrite	1.1	0.5
Primary porosity	8.0	2.2
Secondary porosity	3.2	0.9

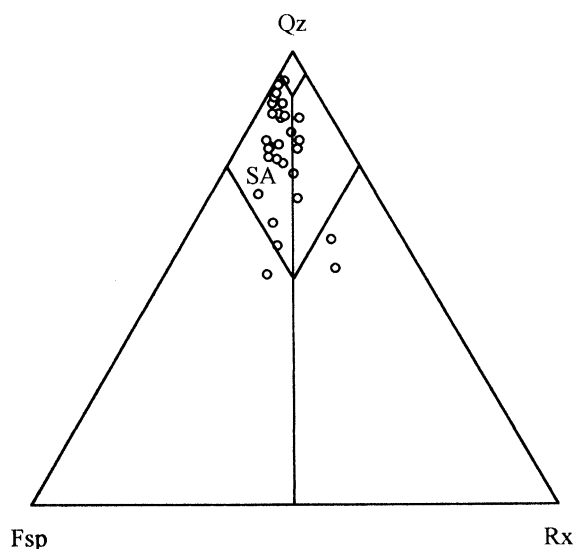


Fig. 2. Ternary plot of sandstone composition from well CN40. Qz: quartz, Fsp: feldspar, Rx: rock fragments, and SA: sub-arkose.

after feldspars is filled with a non-fluorescent oil or bitumen. These hydrocarbon signatures are observed throughout the reservoir, and not just in the present-day oil-leg, though the intensity of fluorescence is greater in the oil-leg than in

the water-leg. Quartz overgrowths are present in the majority of the samples, but are never abundant (mean  $1.7 \pm 0.9\%$ ). Quartz overgrowths are observed to grow around the kaolin (both morphologies; Fig. 3) and are hence interpreted to post-date the kaolin growth and recrystallisation. There is no obvious relationship between quartz overgrowth abundance and burial depth (Fig. 4).

Stable isotopic analyses of authigenic minerals are listed in Table 2. Stable oxygen isotope data for kaolin are plotted versus depth in Fig. 5, note the strong correlation between depth and oxygen isotopic composition. If the data are taken as a whole, then the correlation coefficient ( $R^2$ ) is 0.58, which for 23 points is significant at any reasonable level of confidence. Also note that the data from well CN40 fall on the same correlation line as the two sample sets from well 211/21-14S1. SEM examination of the kaolin separates shows that the 2–5  $\mu\text{m}$  and  $<2 \mu\text{m}$  samples are predominantly blocky crystals, while the 0.1–0.5  $\mu\text{m}$  samples are (somewhat surprisingly) platy crystals suggestive of disaggregated verms. SEM examination of chip samples shows the verms to be substantially larger than the blocky crystals (ca. 10  $\mu\text{m}$  maximum dimension, Fig. 3a), suggesting that the 0.1–0.5  $\mu\text{m}$  samples are probably an early growth stage of the blocky crystals rather than disaggregated verms.

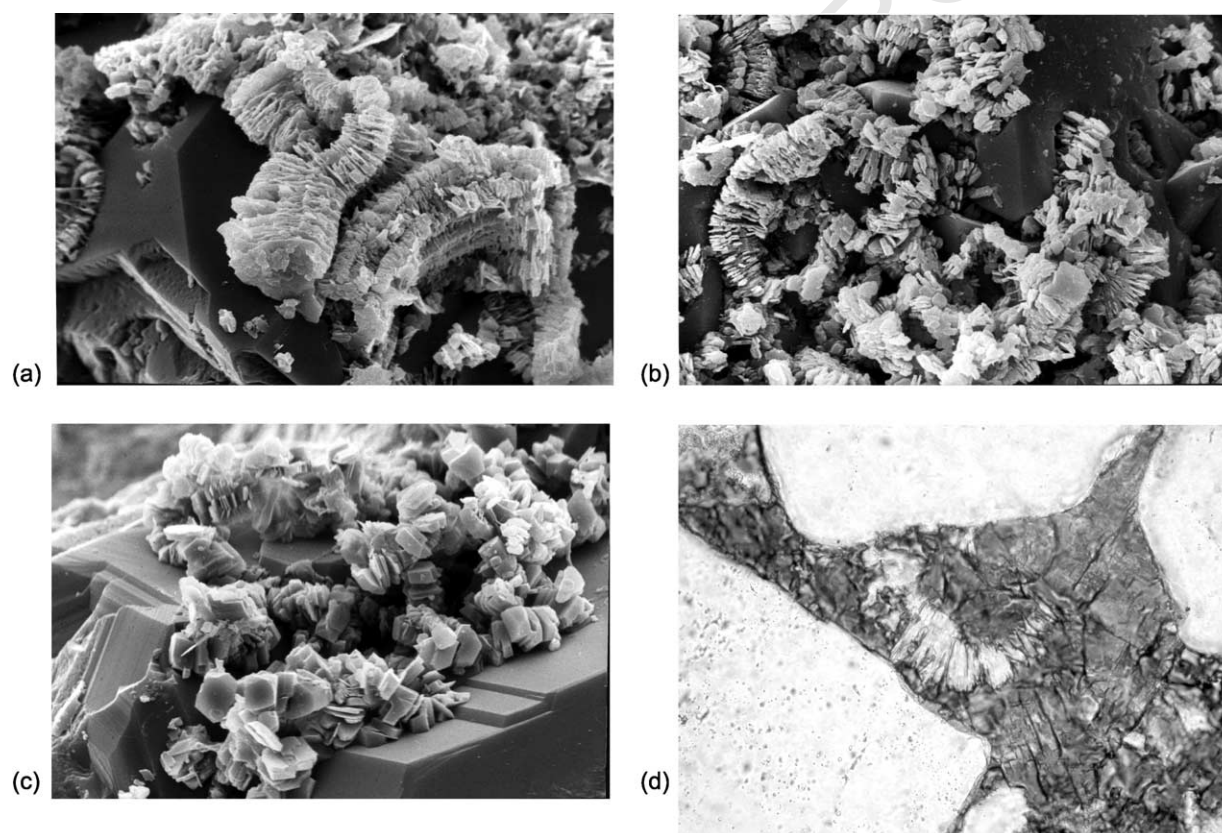


Fig. 3. Kaolin morphologies. (a) Early vermiform crystals (FOV = 55  $\mu\text{m}$  width) which progressively dissolve, (b) while the blocky kaolin crystals grow within the spaces in the verms (FOV = 55  $\mu\text{m}$  width), until (c) only blocky crystals remain (FOV = 110  $\mu\text{m}$  width), (d) the vermiform kaolin is early in the paragenetic sequence as it occurs as a minor phase enclosed within some early calcite concretions (FOV = 275  $\mu\text{m}$  width). There is no visible porosity in this photomicrograph, the spaces between the three quartz grains is entirely filled with an early ferroan dolomite cement which has been stained dark blue for identification purposes.

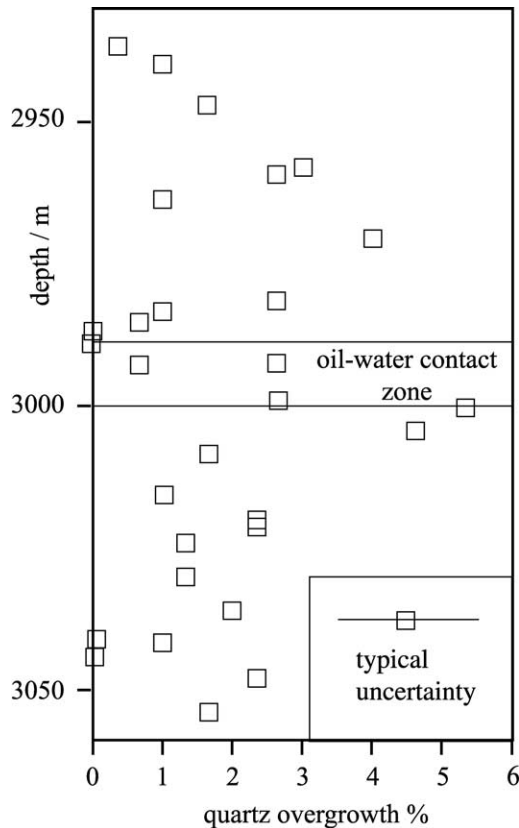


Fig. 4. Abundance of quartz overgrowths versus depth in well CN40, measured by point-counting thin-sections using optical methods. There is no apparent correlation between depth and overgrowth abundance, suggesting that oil-filling was rapid compared to the rate of overgrowth formation. Neither is there more quartz overgrowth below the oil–water contact, suggesting that final oil-filling was relatively recent.

The oxygen isotopic data for the 0.1–0.5  $\mu\text{m}$  samples lie on the same depth trend as that for the remaining data (Fig. 5). Quartz overgrowths are not very abundant in Cormorant IV (generally  $<2\%$ ), due to the relatively shallow depths of burial (2880–3060 m). Only samples from well 211/21-14S1 yielded sufficient overgrowths for analysis, with an average  $\delta^{18}\text{O} = 17.6 \pm 0.3\%$  V-SMOW (Table 2).

Out of six samples processed for illite, only one yielded sufficient sample for a reliable analysis. Other samples were either too small or were heavily contaminated by detrital K-feldspar, which makes reliable analysis impossible. The one good sample from 2946.1 m depth in well 211/21-14S1 yielded an age of  $60.3 \pm 2.0$  Ma. The scarcity of recovered illite presumably reflects the low abundance of illite, though this is difficult to reconcile with the description of Hamilton et al. (1992) of ‘substantial illite growth from 75 °C’ within areas I–III of the Cormorant Field. SEM examination of chip samples from Cormorant IV show that illite is not particularly abundant. Why there should be less illite in Cormorant IV compared to the adjacent Cormorant I–III is unknown. All are at similar burial depths.

Table 3 shows the  $\delta^{18}\text{O}$  and  $\delta\text{D}$  results for the DST water sample for well 211/21-9S1. An attempt to correct

the results for seawater contamination using major-element analyses resulted in a correction that was less than the analytical uncertainty. The best estimate of the present-day porewater composition is  $\delta^{18}\text{O} = -0.6 \pm 0.3\%$  and  $\delta\text{D} = -25 \pm 1\%$  V-SMOW. Aqueous fluid inclusion homogenisation temperatures within quartz overgrowths range from 68 to 116 °C, with a mean of  $96 \pm 2$  °C (Table 4). No pressure correction has been applied as clathrates were observed in many of the inclusions, indicating that the fluids within the inclusions are saturated with methane (Hanor, 1980). Only a very small number of petroleum inclusions were observed, and none are sufficiently large to attempt the measurement of homogenisation temperature ( $<5$   $\mu\text{m}$  diameter). The inclusions fluoresce the same yellow–white colour as the oil-stained clays, described above.

#### 4. Discussion

Previous work on the diagenetic history of the Brent Group has paid little attention to the timing of hydrocarbon emplacement, and the potential effects upon mineral reactions. Giles et al. (1992), for example, presented a detailed paragenetic sequence for the Brent Group that omits to show hydrocarbon emplacement. Where emplacement is shown, it is invariably the last event (Haszeldine et al., 1992; Osborne et al., 1994) with a clear implication that it is unimportant in determining the course of mineral reactions, except perhaps to halt diagenesis entirely. Below, we discuss the hypothesis that oil emplacement occurred relatively early in the burial history of Cormorant IV, and had important interactions with on-going diagenetic reactions. We propose that the correlation between burial depth and  $\delta^{18}\text{O}$  of blocky kaolin is due to kaolin recrystallisation during oil filling of the reservoir (Fig. 6).

Giles et al. (1992) also recognised two phases of kaolin precipitation within the Brent Group, with vermiform kaolin growing at less than 40 °C, and this kaolin recrystallising to a blocky morphology at 90–100 °C. In the present study, we estimate the temperature of recrystallisation of the kaolin as 45–70 °C, using oxygen isotope data (see below). Our temperature estimate is close to that derived by Osborne et al. (1994) in a multi-field isotopic study of kaolin in the Brent Group. They also observed two kaolin morphologies, a vermiform crystal aggregate that grew at less than 50 °C, and replacive blocky crystals formed at between 30 and 80 °C.

The kaolin from Cormorant IV is broadly similar to that described in the studies cited above, i.e. there is an early vermiform kaolin which transforms, apparently by a dissolution–reprecipitation mechanism, into a blocky morphology. The range of measured  $\delta^{18}\text{O}$  of kaolin from Cormorant IV is also similar to previous data sets: 12.9–16.5‰ V-SMOW compared to 13.0–15.4‰ V-SMOW for McAulay, Burley, Fallick, and Kuszniir (1994) and

Table 2

Stable isotope data of authigenic minerals

Well	Formation	Depth (m)	Mineral	Grain size ( $\mu\text{m}$ )	$\delta^{18}\text{O}\text{‰ V-SMOW}$
211/21-14S1	Tarbert	2881.7	Kaolin	2–5	16.5
211/21-14S1	Upper Ness	2899.8	Kaolin	0.1–0.5	16.1
211/21-14S1	Lower Ness	2922.5	Kaolin	2–5	15.6
211/21-14S1	Etive	2928.5	Kaolin	2–5	15.5
211/21-14S1	Etive	2928.7	Kaolin	0.1–0.5	16.0
211/21-14S1	Etive	2938.7	Kaolin	2–5	14.5
211/21-14S1	Etive	2938.9	Kaolin	0.1–0.5	16.5
211/21-14S1	Rannoch	2946.1	Kaolin	2–5	14.1
CN40	Tarbert	2936.8–2947.3	Kaolin	<2	14.3
CN40	Tarbert	2936.8–2947.3	Kaolin	2–5	14.8
CN40	Upper Ness	2954.8–2971.4	Kaolin	<2	14.5
CN40	Upper Ness	2954.8–2971.4	Kaolin	2–5	15.4
CN40	Upper Ness	2982.4–2987.5	Kaolin	<2	13.6
CN40	Upper Ness	2982.4–2987.5	Kaolin	2–5	13.3
CN40	Lower Ness	3001.5–3001.9	Kaolin	<2	12.9
CN40	Lower Ness	3001.5–3001.9	Kaolin	2–5	14.1
CN40	Lower Ness	3006.1–3009.2	Kaolin	2–5	14.2
CN40	Etive	3017.2–3022.6	Kaolin	<2	14.6
CN40	Etive	3017.2–3022.6	Kaolin	2–5	14.8
CN40	Etive	3026.2–3038.2	Kaolin	<2	13.6
CN40	Etive	3026.2–3038.2	Kaolin	2–5	14.1
CN40	Rannoch	3044.5–3046.8	Kaolin	<2	13.4
CN40	Rannoch	3050.2–3056.5	Kaolin	<2	13.2
CN40	Rannoch	3050.2–3056.5	Kaolin	2–5	13.2
211/21-14S1	Upper Ness	2899.7	Quartz overgrowths	5–10	17.1
211/21-14S1	Upper Ness	2899.7	Quartz overgrowths	5–10	17.9
211/21-14S1	Upper Ness	2899.7	Quartz overgrowths	5–10	17.5
211/21-14S1	Upper Ness	2899.7	Quartz overgrowths	5–10	18.0
211/21-14S1	Upper Ness	2899.7	Quartz overgrowths	5–10	17.8
211/21-14S1	Upper Ness	2899.7	Quartz overgrowths	5–10	17.4

12.3–18.5‰ V-SMOW for Osborne et al. (1994). However, the Cormorant IV data shows a unique feature: a decrease in  $\delta^{18}\text{O}$  with depth (Fig. 5). There is a displacement in the data at 3015 m, which is apparent in both grain-size separates, the significance of which is discussed below. We propose that the depth- $\delta^{18}\text{O}$  correlation is due to the recrystallisation of kaolin synchronous with oil filling (referred to as the oil-filling model). However, we will also discuss three alternative models for kaolin recrystallisation, each with a different explanation for the depth- $\delta^{18}\text{O}$  correlation. Only two variables can be responsible for variation in  $\delta^{18}\text{O}$ : temperature and porewater oxygen isotopic composition ( $\delta^{18}\text{O}$ ). Four possible explanations are proposed for the depth- $\delta^{18}\text{O}$  correlation.

Firstly, the oil-filling model: kaolin recrystallisation took place during oil emplacement (Fig. 6), with recrystallisation being stopped, or at least retarded, within the filled (uppermost) portions of the field. The kaolin at the top of the field would be younger (lower temperature, higher  $\delta^{18}\text{O}$ ) than the kaolin lower down. Secondly, it could be a physical mixing line between late blocky (low  $\delta^{18}\text{O}$ ) and early vermiform (high  $\delta^{18}\text{O}$ ) kaolin. This is rejected as SEM studies showed all the kaolin separates to be of predominantly blocky morphology. Thirdly, the kaolin could have recrystallised at a time of extremely high geothermal

gradient, or fourthly, the oxygen isotopic composition of the porewaters could have varied with depth, i.e. the kaolin recrystallised in stratified porewaters. The options one, three and four are discussed below.

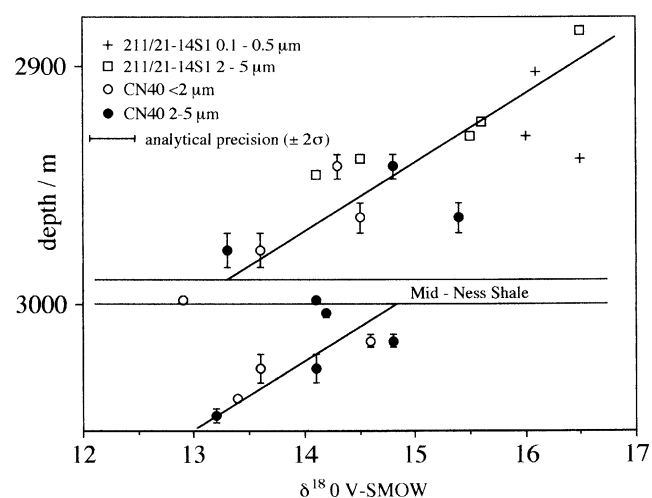


Fig. 5. Stable oxygen isotope ratio of authigenic kaolin versus burial depth. Note the linear correlation, with an offset at ca. 3000 m depth which corresponds to a low-permeability unit, the Mid-Ness shale. This shale coincides with the modern oil–water contact in well CN40, but not in 211/21-14S1. Data from both wells apparently lie along the same trend, although the wells are approximately 3 km apart.

Table 3  
Stable isotope data for drill stem test water sample (well 211/21-9S1)

$\delta^{18}\text{O}\text{‰ SMOW}$	$\delta\text{D}\text{‰ V-SMOW}$
0.2	-26
-0.4	-25
-1.0	-27
-0.6	
-1.2	-24
-0.9	
-0.6	-25

Table 4  
Homogenisation temperatures of aqueous fluid inclusions in quartz from well CN23

Depth (m)	$T_h$ (°C)	Max length ( $\mu\text{m}$ )	Notes
2845.7	89.2	6	Quartz healed fracture
2845.7	93.9	5	Quartz healed fracture
2845.7	88.9	3	In quartz at boundary of dust rim and overgrowth
2845.7	105	2	In quartz at boundary of dust rim and overgrowth
2845.7	106	2	In quartz at boundary of dust rim and overgrowth
2845.7	95	8	At boundary of dust rim and quartz overgrowth
2845.7	67.7	2	At boundary of dust rim and quartz overgrowth
2845.7	107.1	2	In quartz overgrowth at dust rim
2845.7	106.8	3	In quartz overgrowth at dust rim
2845.7	102.6	6	In quartz overgrowth out from dust rim
2845.7	116	2	In quartz cement
2845.7	115	2	In quartz cement
2845.7	96.5	4	In quartz overgrowth out from dust rim
2845.7	104.3	8	In middle of quartz overgrowth
2845.7	101.7	6	In quartz cement
2845.7	89.6	6	Near outer edge of quartz overgrowth
2845.7	92.6	3	In quartz cement
2845.7	96.7	4	In quartz cement
2845.7	85.6	4	In quartz overgrowth
2845.7	107	30	In middle of quartz overgrowth
28 45.7	81.6	4	In healed quartz fracture pre-dating overgrowth
2845.7	80.3	7	In healed quartz fracture pre-dating overgrowth
2845.7	78.1	3	In healed quartz fracture pre-dating overgrowth
2876.2	98	3	At boundary of dust rim and quartz overgrowth
2876.2	97.5	4	At boundary of dust rim and quartz overgrowth
2876.2	105	15	At boundary of dust rim and quartz overgrowth

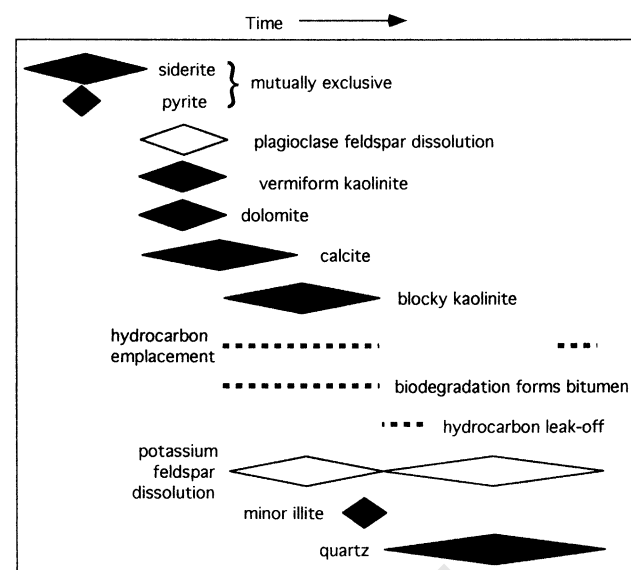


Fig. 6. Paragenetic sequence for the Cormorant Field. Dissolution events are shown as clear symbols.

#### 4.1. The 'geothermal gradient' model

Could the kaolin  $\delta^{18}\text{O}$ -depth correlation be due simply to the ambient geothermal gradient at the time of kaolin recrystallisation? Calculation shows that if the entire variation in  $\delta^{18}\text{O}$  were due to temperature change, then a geothermal gradient of ca. 180 °C/km would be implied. A high geothermal gradient 'event' within the East Shetland Basin can be dismissed conclusively. The present-day geothermal gradient is only 30–35 °C/km (unpublished sub-surface temperature measurements, Shell Expro UK). There is no evidence of any igneous activity within the area, and no previous reports of anomalously high isotopic mineral 'temperatures,' fluid inclusion values, or vitrinite-reflectance data. As the East Shetland Basin has been exhaustively explored for its hydrocarbon resources, it is unlikely that such evidence could have been missed entirely. Any igneous intrusion underlying the Cormorant reservoir would probably have been revealed by seismic imaging of the oil-bearing structures. Moreover, the offset in the  $\delta^{18}\text{O}$ -depth correlation at ca. 3015 m could not be easily explained by the geothermal gradient model. We hence reject the possibility that the  $\delta^{18}\text{O}$ -depth correlation for kaolin was due to an enhanced geothermal gradient at the time of kaolin recrystallisation.

#### 4.2. The 'layered porefluids' model

In the Magnus Field, which lies some 50 km from Cormorant IV, Macaulay, Haszeldine, and Fallick (1992) used isotopic evidence to show that the porewaters were stratified for much of the burial history. To apply a similar model to Cormorant IV, it is necessary to propose that relatively low  $\delta^{18}\text{O}$  water must have been present in the base of the structure, and higher  $\delta^{18}\text{O}$  water at the top, with an

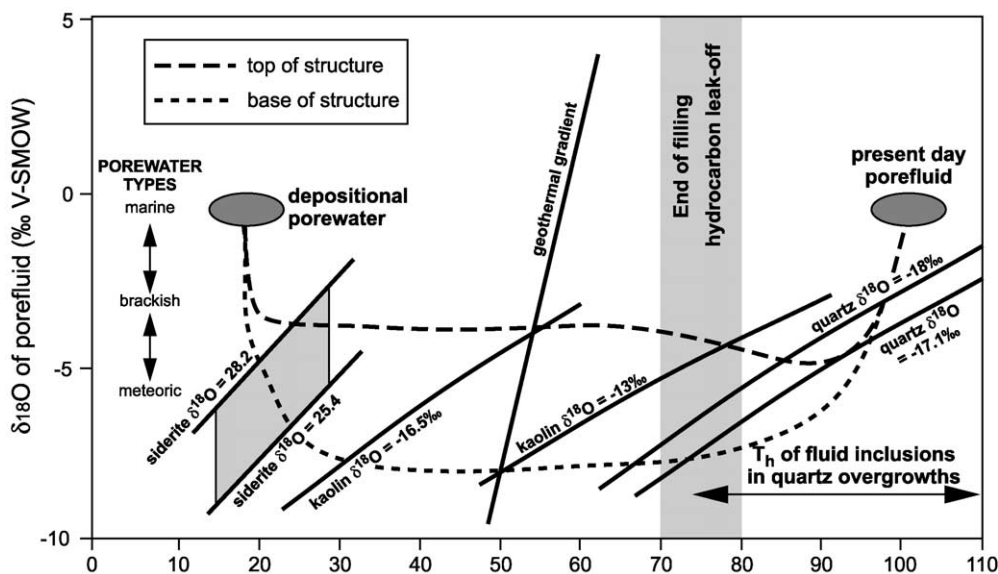


Fig. 7. Suggested porewater evolution curves for the 'layered-porefluids' model. This model is here rejected in favour of the 'oil-filling' model. In the 'layered porefluids' model, the porefluids within the sandstone are inhomogeneous, with low  $\delta^{18}\text{O}$  fluids at the base of the structure, and higher  $\delta^{18}\text{O}$  fluids at the top. It is proposed that the low  $\delta^{18}\text{O}$  fluids entered the base of the sandstones, possibly from the adjacent Triassic sandstones, and evolved to higher  $\delta^{18}\text{O}$  compositions due to mixing as they ascended. The kaolin growth is shown as occurring at 50–55 °C, though higher temperatures could also be accommodated.

approximately linear gradation except for at 3015 m depth where an offset is apparent in the kaolin data (Fig. 5). A recrystallisation temperature of 30–100 °C is implied (Giles et al., 1992; Osborne et al., 1994), with a preferred range of 50–75 °C (this study). Fig. 7 shows the proposed relationships between recrystallisation temperature, porewater composition and  $\delta^{18}\text{O}$  of the blocky kaolin for the layered porefluids model

It is difficult to imagine how layered porewater could be maintained for geological periods of time, in a highly porous and permeable sandstone in which both diffusion and any fluid advection would cause fluid homogenisation. One explanation is to have a supply of low  $\delta^{18}\text{O}$  water introduced continuously into the lower parts of the structure, and mixing as it ascended with connate, or other, higher  $\delta^{18}\text{O}$  waters. de Caritat and Baker (1992) proposed just such a hydro-geological scheme to account for an anomalous range in  $\delta^{18}\text{O}$  measured in ankerite from the Aldebaran Sandstone of Queensland, Australia. They used numerical modelling to show that a combination of an enhanced geothermal gradient caused by upward movement of fluid, and the effect of introducing low  $\delta^{18}\text{O}$  fluids, could account for a change in  $\delta^{18}\text{O}$  in the precipitated ankerite of approximately 6‰ over around 700 m. Fig. 7 shows that this hypothesis is not compatible with recrystallisation of kaolin in Jurassic meteoric porewaters typical of Northern Scotland ( $\delta^{18}\text{O} = -5$  to  $-7$ ‰, SMOW, Hudson & Andrews, 1987), unless recrystallisation was at the lower limits of the probable temperature range (ca. 50 °C), when fluids which were slightly more depleted in  $^{18}\text{O}$  would have to be involved. The proposed porewater evolution curves for the lower part of the Cormorant IV structure (Fig. 7) are broadly comparable

with those published by Haszeldine et al. (1992) for the Dunlin, Thistle and Murchison fields which lie some 30–40 km to the east of Cormorant IV.

One problem with this model is that a through-flow of water is required. However, it is clear that the Cormorant structure is capable of trapping oil, such that any fluid flow must be quite limited. Furthermore, this model cannot easily account for the 2‰ offset in oxygen isotopic composition of kaolin at ca. 3015 m depth (Fig. 5), unless two mixing systems are proposed, one above and one below the Mid-Ness Shale. For these reasons, we reject the layered porefluid model as an explanation for the  $\delta^{18}\text{O}$  of kaolin-depth correlation.

#### 4.3. The 'oil-filling' model

This is our preferred model for the depth- $\delta^{18}\text{O}$  correlation. Kaolin recrystallisation could only be affected gradationally by hydrocarbon emplacement if recrystallisation and hydrocarbon filling were synchronous. It is difficult to directly date the timing of oil filling in Cormorant IV, however, as it has been proposed that authigenic illite in the Brent Group grew at the time of trap filling (Hamilton et al., 1992), the K–Ar dating of illite provides a possible solution. Unfortunately, only a single illite age of  $60.3 \pm 2.0$  Ma has been obtained from Cormorant IV, from an oil-filled zone. In the adjacent, structurally higher, areas of the Cormorant field (designated Cormorant I–III), illite has been dated as  $35 \pm 1$  and  $41 \pm 1$  Ma within a water-filled zone (Hamilton et al., 1992). Here, detrital contamination was identified as a potential problem, so that the true age of the illite may be younger than the analytical result. Hamilton et al. (1992) noted that the immediately overlying Kimmeridge Clay

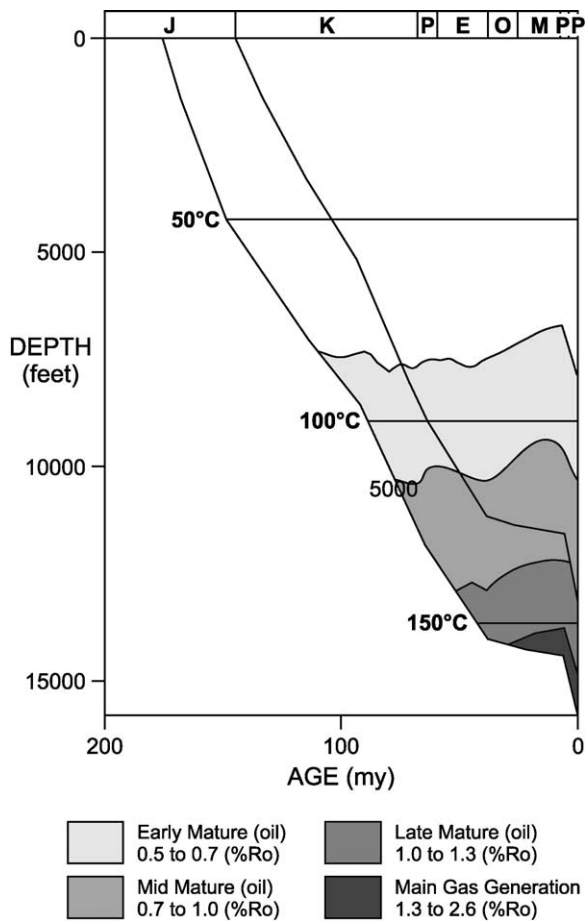


Fig. 8. Basin model of a pseudo-well located in the deepest part of a potential kitchen area due east of Cormorant IV. It shows that hydrocarbons were being generated from mid-Cretaceous times onwards, and that it is realistic to have kaolin growth (80–40 Ma) as synchronous with hydrocarbon charging into the reservoir. The stratigraphy of the model is constructed using a 2D seismic section supplied by Shell UK. The thermal history is very simplistic, as there is no data available to calibrate the model. Default values of heat-flows and thermal parameters were used from BasinMod™.

formation was immature with respect to oil generation at the time of apparent illite growth, since the Brent Group itself was at only 75 °C. However, the Cormorant structure lies immediately west of a structural low, in which a considerable thickness of Kimmeridge clay can be identified (unpublished seismic data, Shell Expro). The thermal history of the sediments of this potential kitchen has been modelled using a 1D code (BasinMod™, Fig. 8). Although the thermal model used is very simplistic, and uses mostly default parameters (as there are no data from the kitchen area to calibrate the model to), the results support the hypothesis that the illite ages of Hamilton et al. (1992) record oil filling in the Cormorant structure, as the illite ages coincide with peak maturity in the potential source rocks. Previous work has indicated first oil generation at 65 Ma, and peak generation during the Paleogene (Taylor & Dietvorst, 1991). This latter result is probably representative of the deeply buried source rocks within the Viking Graben,

which lies immediately to the east of the East Shetland Platform (Fig. 1). Hence, the field may have been involved in a long and multi-stage history of filling and migration.

Hamilton et al. (1992) made a detailed study of illite K–Ar ages in the Brent Group, and concluded that illite ages are related to oil filling. Ages from the water-leg of the reservoir were thought to immediately post-date filling. Hence, we use K–Ar ages of illite from Cormorant as probable indicators of the cessation of field filling and use the single oil-leg age (this study) as an indication of time of oil-filling ( $60.3 \pm 2.0$  Ma). Using the burial history of Hamilton et al. (1992) implies oil emplacement at maximum temperatures of 70–80 °C. This is also the maximum temperature at which biodegradation can occur, to form the bitumen observed in thin-sections. Fig. 9 shows that temperatures of 70–80 °C are consistent with kaolin recrystallisation from Jurassic meteoric porewaters ( $\delta^{18}\text{O} = -5$  to  $-7\text{‰}$  V-SMOW), and fit well with data from siderite (Wilkinson et al., 2000) and quartz overgrowths (Tables 3 and 4). The porefluid evolution shown is comparable to that of Haszeldine et al. (1992), which was proposed for the Dunlin, Thistle and Murchison fields. These fields lie some 30–40 km to the east of Cormorant IV. Note that the present-day porewater in Cormorant IV has considerably heavier  $\delta^{18}\text{O}$  values than Jurassic meteoric water. Haszeldine et al. (1992) proposed that the East Shetland Basin had a zoned paleo-hydrogeology, with active meteoric water recharge down to a depth corresponding to a temperature of 80–90 °C. Below this were static ‘basinal’ porewaters with  $\delta^{18}\text{O}$  of greater than 0‰ SMOW. Our results support this model, and imply that the first hydrocarbon charge would have been emplaced within the actively recharging, meteoric water aquifer, portion of the basin. This might be expected to lead to the formation of bitumen, due either to water washing, or to bio-degradation of the oil due to the low ambient temperatures (Lomando, 1992). Bitumen is observed within thin-sections, even within the present-day water-leg, and is especially prominent within secondary pores developed in potassium feldspars.

There is one observation that does not seem to fit the oil-filling hypothesis. Some of the blocky kaolin samples were taken from the present-day water-leg of the reservoir, and the  $\delta^{18}\text{O}$ -depth trend is apparent here (well CN40) as well as in the present-day oil-leg (Fig. 5). We propose that, in the past, this lower zone of the reservoir was oil-filled, and that the oil has subsequently leaked off into the overlying formations. Such filling and emptying of reservoirs over geological time periods are a widespread phenomenon (Bhullar, Karlsen, Backer-Owe, Seland, & LeTran, 1999; Heasley et al., 2000). Direct evidence for the former presence of oil in the lower section of the reservoir is provided by very rare minute oil inclusions trapped within quartz overgrowths, and the yellow–white fluorescence in ultra-violet light of pore-filling clays. The colour of the fluorescence is the same as observed in the oil-filled sections

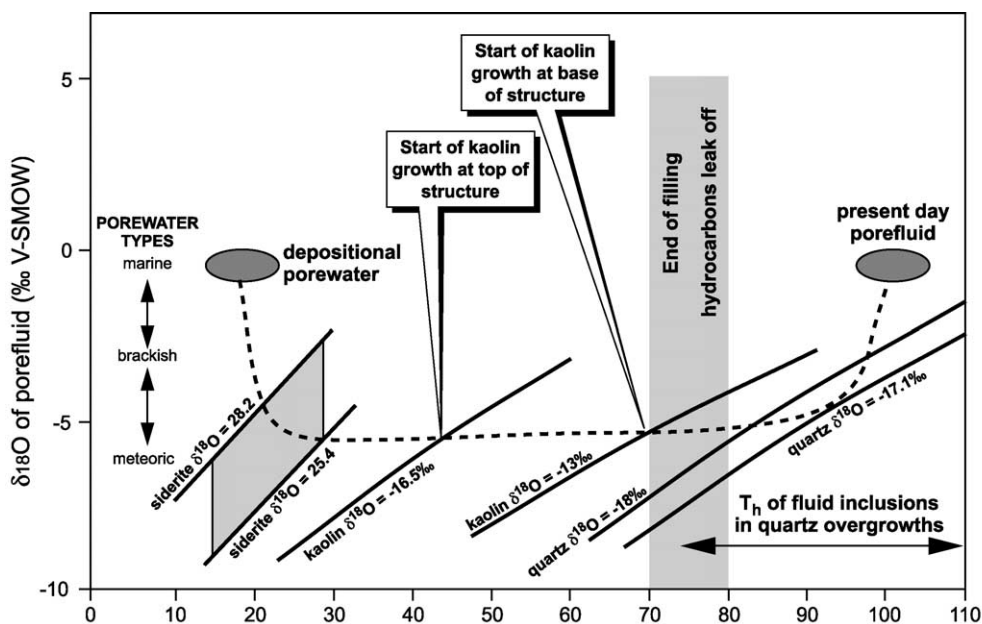


Fig. 9. Suggested porewater evolution curve for the 'oil-filling' model. The porewaters within the sandstone are homogeneous at any given time, but evolve during kaolin growth, which is simultaneous with oil filling. Kaolin growth begins at ca. 45 °C in porewaters of meteoric origin, and ends at the completion of oil filling. The early kaolin at the top of the structure is preserved as oil filling prevents or retards further growth. The porefluid evolution curve is constrained by isotopic data from siderite and quartz overgrowths which were extracted from other wells in Cormorant IV, though the proposed curve is not a unique solution.

of the reservoir, but less intense. The fluorescence is interpreted as due to adsorbed hydrocarbon on the clay surfaces.

The  $\delta^{18}\text{O}$ -depth correlation shows an offset of 2‰ at ca. 3015 m depth (Fig. 5). This corresponds to a regional shale unit, the Mid-Ness shale. This regionally extensive 4–6 m thick shale might be expected to have acted as a barrier to vertical fluid migration (as at present-day, Howe, 1992), causing oil to accumulate below it during filling despite the presence of water-filled sandstone above the shale. Hence, in the 'oil-filling' model, the offset in the  $\delta^{18}\text{O}$ -depth correlation at ca. 3015 m depth represents local oil pooling below the Mid-Ness shale.

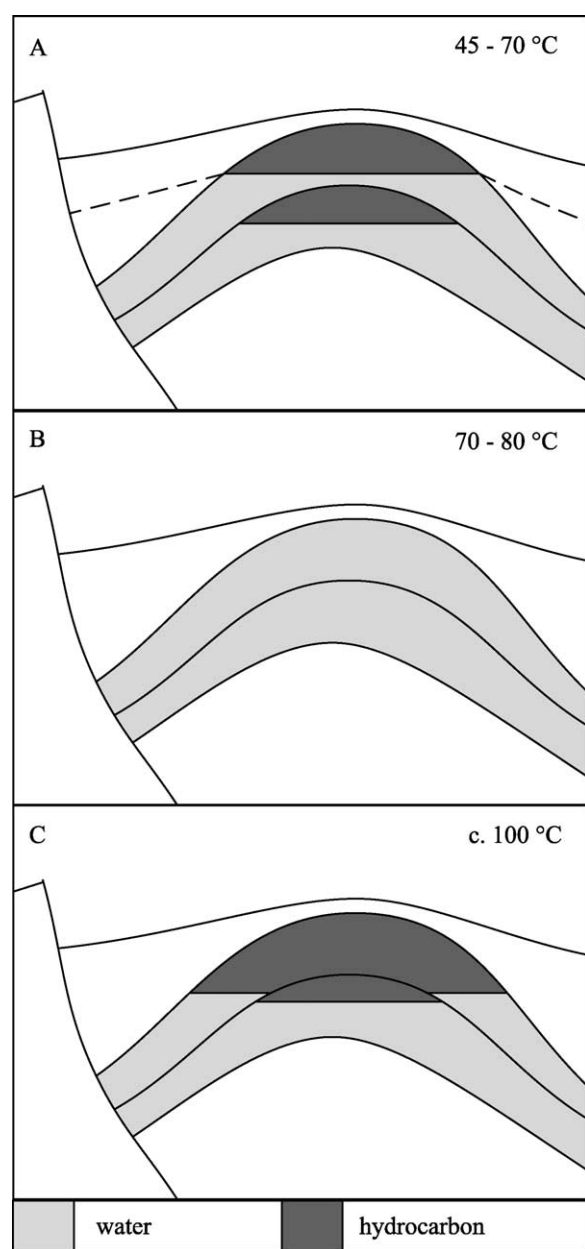
The timing of hydrocarbon leakage from Cormorant IV is poorly constrained. However, the fluid inclusions from quartz overgrowths are predominantly filled with aqueous fluids, and record quartz growth in the present-day water-leg, presumably in the absence of high concentrations of hydrocarbons, i.e. after leak-off. As the fluid inclusions record temperatures of 68–116 °C, the present-day water-leg must have lost the hydrocarbon column soon after the completion of the initial filling episode (Fig. 9). Quartz overgrowths have formed throughout the reservoir sandstones, and could only have formed after the interpreted initial oil filling, as the temperatures were too low before filling. The minimum temperature at which quartz overgrowths are commonly formed is ca. 80 °C (Giles et al., 1992), and the first hydrocarbon is interpreted to have filled the reservoir at a lower temperature. In order to produce uniform quartz overgrowths throughout the reservoir (Fig. 4), there must have been a significant period of time

in between leak-off of the first hydrocarbon charge, and the arrival of the second (present-day) charge. Assuming that the quartz overgrowths were still forming when the second oil-filling began, then it might be expected that the abundance of quartz overgrowths would increase with increasing depth within the reservoir, due to top-down filling causing the cessation of quartz overgrowth formation at the crest of the field first, and only later at lower levels (Marchand et al., 2001, 2002). Such a pattern in the abundance of quartz overgrowths is not observed (Fig. 4), for which the most likely explanation is that filling was rapid compared to the rate of formation of quartz overgrowths. In addition, the measurement of quartz overgrowth abundance by conventional optical methods is not very accurate, especially when low abundances are being point-counted. Hence, any subtle variation in the abundance of quartz overgrowths with depth might easily be missed. Secondly, there is a range of sandstone facies within the Brent Group, and the rate of formation of quartz overgrowths will vary from facies to facies. Both of these factors will tend to obscure any pattern in overgrowth abundance.

Why did not the recrystallisation of kaolin continue after the loss of the early hydrocarbon charge? The most likely explanation is that all of the oil was not flushed from the sandstone, but that some was left, particularly coating grain surfaces. Polar oil molecules have a preference for clay surfaces (Larter et al., 1996), as these have a residual surface charge. Hence the residual oil would have been preferentially left upon the kaolin. This would effectively isolate the (oil-wet) kaolin from the porewater, and prevent further recrystallisation. Quartz and feldspar surfaces would have

1121 been left more water-wet, allowing processes such as the  
1122 formation of quartz overgrowths to continue relatively  
1123 unimpeded.

1124 All previous published diagenetic histories of Brent  
1125 Group reservoir have assumed that oil emplacement was  
1126 the last event to have occurred (Haszeldine et al., 1992;  
1127 Osborne et al., 1994) or have omitted hydrocarbon  
1128 emplacement as a diagenetic event, presumably with the  
1129 implication that hydrocarbon emplacement had little or no  
1130



1171 Fig. 10. Summary of the filling history of the Cormorant IV field. (A) The  
1172 initial hydrocarbon charge has two oil-pools separated by a regionally  
1173 extensive shale barrier (the Mid-Ness Shale, MNS). Filling is contempora-  
1174 neous with the growth of authigenic kaolin. (B) Complete leak-off allows  
1175 diagenesis to continue, especially the formation of quartz overgrowths,  
1176 which trap fluid inclusions. (C) The present-day oil charge is the last event  
1177 in the field history.

1177 influence upon diagenetic reactions in this instance (Giles  
1178 et al., 1992). The reconstruction of diagenetic events  
1179 presented in this paper shows that hydrocarbon emplace-  
1180 ment occurred relatively early in the history of the  
1181 reservoir, and was synchronous with the recrystallisation  
1182 of kaolin (Fig. 6). Other reactions, such as the formation of  
1183 quartz overgrowths, occurred only after the initial hydro-  
1184 carbon charge had leaked off. Given the large volume of  
1185 work that has been carried out on the Brent Group fields in  
1186 the East Shetland Basin, it is perhaps surprising that no  
1187 other workers have suggested interaction between hydro-  
1188 carbon fluids and diagenetic processes. As an illustration,  
1189 comparing the diagenetic history of Giles et al. (1992) with  
1190 the likely hydrocarbon generation times in Taylor and  
1191 Dietvorst (1991), it is apparent that the majority of the  
1192 diagenesis is supposed to have occurred after peak  
1193 hydrocarbon generation. It remains to be seen how  
1194 applicable the proposed filling history for Cormorant IV  
1195 is to other Brent Group fields.

1196 In summary, the oil-filling model is the preferred  
1197 explanation for the  $\delta^{18}\text{O}$ -depth correlation (Fig. 10). It  
1198 has also the advantage of being compatible with previous  
1199 diagenetic studies in the area, and of inherent simplicity.  
1200 It does require that there was previously a hydrocarbon  
1201 column that was substantially greater than the present-  
1202 day fill. However, there is sufficient independent  
1203 evidence for the previous presence of oil within the  
1204 present-day water-leg (minute hydrocarbon-filled  
1205 inclusions, oil-stained clays) to justify this. In addition,  
1206 biodegraded oil is found in some Brent Fields (Bhullar  
1207 et al., 1999; Horstad et al., 1990). Given that biode-  
1208 gradation is halted at around 70–80 °C, this is good  
1209 evidence for early oil charging. Early oil leak-off and  
1210 replacement with a recent charge has also been described  
1211 (Bhullar et al., 1999).  
1212

## 1213 5. Conclusions

- 1214 1. The Cormorant IV reservoir is interpreted to have been  
1215 filled by hydrocarbons from 80 to 40 Ma, interrupting  
1216 diagenetic reactions within the oil-leg. There were two  
1217 oil pools, one above and one below the Mid-Ness Shale,  
1218 a regionally extensive low-permeability unit that divides  
1219 the Brent Group. The hydrocarbons subsequently leaked  
1220 off, allowing diagenesis to continue throughout the  
1221 reservoir, until the present-day oil charge was emplaced  
1222 as the last event in the reservoir history (Fig. 10). This  
1223 sequence of events is more complex than has been  
1224 previously assumed, and has been reconstructed using  
1225 diagenetic evidence.  
1226
- 1227 2. There are two morphologies of kaolin in Cormorant IV,  
1228 an early vermiform and a later blocky kaolin. The  
1229 blocky kaolin is formed by the recrystallisation of the  
1230 vermiform kaolin. All the kaolin samples prepared for  
1231 isotopic analysis consisted of the later, blocky kaolin.  
1232

- 1233 3. There is a strong correlation between  $\delta^{18}\text{O}$  of blocky  
 1234 kaolin and depth for kaolin samples from two wells  
 1235 from the Cormorant Field, with a 2‰ offset corre-  
 1236 sponding to the Mid-Ness Shale. The correlation is  
 1237 interpreted as due to kaolin recrystallisation during  
 1238 hydrocarbon filling from 45 to 70 °C, at which time  
 1239 modelling of a kitchen area in an adjacent depo-centre  
 1240 shows potential source rocks to be at peak maturity.  
 1241 The Mid-Ness Shale sub-divided the reservoir. Filling  
 1242 ended approximately 60 Ma ago, which is coincident  
 1243 with the single K–Ar age of an illite sample from the  
 1244 water-leg of the field. The (lowermost) oil–water  
 1245 contact at this time is proposed to have been  
 1246 significantly lower in the stratigraphy than the  
 1247 present-day equivalent, as shown by minute oil-bearing  
 1248 inclusions and oil-stained clay within the present-day  
 1249 water-leg. The reservoir was within the zone of active  
 1250 meteoric water recharge, and bitumen was formed by  
 1251 water washing or biodegradation.
- 1252 4. The hydrocarbon which is interpreted to have been  
 1253 initially reservoid in the Cormorant IV structure  
 1254 probably leaked off soon after filling ended, allowing  
 1255 diagenesis to continue in the (new) water-leg (Fig. 10).  
 1256 Quartz overgrowths are the major late diagenetic  
 1257 phase.
- 1258 5. The last event to occur within the reservoir was the  
 1259 influx of the present-day oil charge. This is inferred  
 1260 to have occurred when the reservoir was buried  
 1261 below the zone of active meteoric water recharge in  
 1262 the basin, in the zone of relatively stagnant basinal  
 1263 porefluids (Fig. 10).
- 1264 6. All previous published diagenetic histories of Brent  
 1265 Group reservoir have assumed that oil emplacement  
 1266 was the last event to have occurred. Our reconstruction  
 1267 shows that hydrocarbon emplacement occurred rela-  
 1268 tively early in the history of the reservoir, and was  
 1269 synchronous with some of the diagenetic reactions.  
 1270 Other reactions occurred only after the initial hydro-  
 1271 carbon charge had leaked off. It remains to be seen  
 1272 whether this filling history is applicable to other Brent  
 1273 Group fields in the East Shetland Basin.

#### Acknowledgements

1274  
 1275  
 1276 MW was funded by Shell Expro UK, who provided data,  
 1277 rock and much help. Mineral separation was carried out by  
 1278 Bill Higgison. Stable isotope analyses were carried out by  
 1279 staff at the Scottish Universities Environmental Research  
 1280 Centre. Thanks to Colin Farrow of Glasgow University for  
 1281 the triangular plotting program. Gordon MacLeod carried  
 1282 out the fluid inclusion measurements while at the Newcastle  
 1283 Research Group, University of Newcastle, on inclusion  
 1284 wafers made by John Gilleece. The DTI core store in  
 1285 Edinburgh, Scotland, is thanked for supplying rock for  
 1286 the manufacture of four fluid inclusion wafers, made by

1287 Mike Hall. Platte River Associates (Denver) kindly donated  
 1288 the BasinMod™ software. Reviews by Craig Smalley and  
 1289 Richard Worden improved the clarity of the manuscript.

#### References

- 1290  
 1291  
 1292  
 1293  
 1294  
 1295  
 1296  
 1297  
 1298  
 1299  
 1300  
 1301  
 1302  
 1303  
 1304  
 1305  
 1306  
 1307  
 1308  
 1309  
 1310  
 1311  
 1312  
 1313  
 1314  
 1315  
 1316  
 1317  
 1318  
 1319  
 1320  
 1321  
 1322  
 1323  
 1324  
 1325  
 1326  
 1327  
 1328  
 1329  
 1330  
 1331  
 1332  
 1333  
 1334  
 1335  
 1336  
 1337  
 1338  
 1339  
 1340  
 1341  
 1342  
 1343  
 1344
- Bhullar, A. G., Karlens, D. A., Backer-Owe, K., Seland, R. T., & LeTran, K. (1999). Dating reservoir filling—a case history from the North Sea. *Marine and Petroleum Geology*, *16*, 581–603.
- Bloch, S., Lander, R. H., & Bonnell, L. (2002). Anomalously high porosity and permeability in deeply buried sandstone reservoirs: origin and predictability. *American Association of Petroleum Geologists Bulletin*, *86*, 301–328.
- Brint, J. F. (1989). *Isotope diagenesis and paleofluid movement: Middle Jurassic Brent Sandstones, North Sea*. Unpublished PhD Thesis, University of Glasgow.
- de Caritat, P., & Baker, J. C. (1992). Oxygen-isotope evidence for upward, cross-formational flow in a sedimentary basin near maximum burial. *Sedimentary Geology*, *78*, 155–164.
- Darby, D., Wilkinson, M., Fallick, A. E., & Haszeldine, R. S. (1997). Illite dates record deep fluid movements in petroleum basins. *Petroleum Geoscience*, *3*, 133–140.
- Deighton, I. (1996). *Thermal modelling of the North West shelf (Vol. 1)* (p. 74). Canberra: Australian Geological Society Organisation.
- Demyttenaere, R. R. A., Sluijk, A. K., & Bentley, M. R. (1993). A fundamental reappraisal of the structure of the Cormorant Field and its impact on field development strategy. *Petroleum geology of Northwest Europe: Proceedings of the fourth conference* (pp. 1151–1157). London: Geological Society.
- Donnelly, T., Waldron, S., Tait, A., Dougans, J., & Bearhop, S. (2001). Hydrogen isotope analysis of natural abundance and deuterium-enriched waters by reduction over chromium on-line to a dynamic dual inlet isotope-ratio mass spectrometer. *Rapid Communications in Mass Spectrometry*, *15*, 1297–1303.
- Epstein, S., & Mayeda, T. (1953). Variation of  $^{18}\text{O}$  content of waters from natural sources. *Geochimica et Cosmochimica Acta*, *4*, 213–224.
- Fallick, A. E., Macaulay, C. I., & Haszeldine, R. S. (1993). Implications of linearly correlated oxygen and hydrogen compositions for kaolinite and illite in the Magnus Sandstone, North Sea. *Clays and Clay Minerals*, *41*, 184–190.
- Giles, M. R., Stevenson, S., Martin, S. V., Cannon, S. J. C., Hamilton, P. J., Marshall, J. D., & Samways, G. M. (1992). The reservoir properties and diagenesis of the Brent Group: A regional perspective. In A. C. Morton, R. S. Haszeldine, M. R. Giles, & S. Brown (Eds.), *Geology of the Brent Group* (pp. 289–327). Geological Society, London, Special Publication, *61*.
- Hamilton, P. J., Giles, M. R., & Ainsworth, P. (1992). K–Ar dating of illites in Brent Group reservoirs: A regional perspective. In A. C. Morton, R. S. Haszeldine, M. R. Giles, & S. Brown (Eds.), *Geology of the Brent Group* (pp. 377–400). Geological Society, London, Special Publication, *61*.
- Hamilton, P. J., Kelley, S., & Fallick, (1989). K–Ar dating of illite in hydrocarbon reservoirs. *Clay Minerals*, *24*, 215–231.
- Hanor, J. S. (1980). Dissolved methane in sedimentary brines; potential effects on the PVT properties of fluid inclusions. *Economic Geology*, *75*, 603–617.
- Haszeldine, R. S., Brint, J. F., Fallick, A. E., Hamilton, P. J., & Brown, S. (1992). Open and restricted hydrologies in Brent Group diagenesis: North Sea. In A. C. Morton, R. S. Haszeldine, M. R. Giles, & S. Brown (Eds.), *Geology of the Brent Group* (pp. 401–419). Geological Society, London, Special Publication, *61*.
- Heasley, E. C., Worden, R. H., & Hendry, J. P. (2000). Cement distribution in a carbonate reservoir: recognition of a palaeo oil–water contact and

- 1345 its relationship to reservoir quality in the Humbly Grove field, onshore,  
 1346 UK. *Marine and Petroleum Geology*, 17, 639–654.
- 1347 Honarpour, M., Koederitz, L., & Harvey, A. H. (1986). *Relative*  
 1348 *permeability of petroleum reservoirs*. Boca Raton, FA: CRC Press,  
 1349 143 p.
- 1350 Horstad, I., Larter, S. R., Dypvik, H., Aagaard, P., Bjornvik, A. M.,  
 1351 Johansen, P. E., & Eriksen, S. (1990). Degradation and maturity  
 1352 controls on oil-field petroleum column heterogeneity in the Gullfaks  
 1353 Field, Norwegian North-Sea. *Organic Geochemistry*, 16, 497–510.
- 1354 Howe, B. K. (1992). Cormorant Field; U.K., East Shetland Basin, North  
 1355 Sea. In N. H. Foster (Ed.), *Structural traps VI, Treatise of petroleum*  
 1356 *geology, atlas of oil and gas fields* (pp. 1–35). American Association of  
 1357 Petroleum Geologists.
- 1358 Hudson, J. D., & Andrews, J. E. (1987). The diagenesis of the Great  
 1359 Estuarine group, Middle Jurassic, Inner Hebrides, Scotland. In J. D.  
 1360 Marshall (Ed.), *Diagenesis of sedimentary sequences* (pp. 259–276).  
 1361 *Geological Society Special Publication* 36.
- 1362 Kantorowicz, J. D. (1990). The influence of variations in illite morphology  
 1363 on permeability of Middle Jurassic Brent Group sandstones, Cormorant  
 1364 Field, UK North Sea. *Marine and Petroleum Geology*, 7, 66–74.
- 1365 Larter, S. R., Bowler, B. F. J., Li, M., Chen, M., Brincat, D., Bennett, B.,  
 1366 Noke, K., Donohoe, P., Simmons, D., Kohlen, M., Allan, J., Telnaes,  
 1367 N., & Horstad, I. (1996). Molecular indicators of secondary oil  
 1368 migration distances. *Nature*, 383, 593–597.
- 1369 Lomando, A. J. (1992). The influence of solid reservoir bitumen on  
 1370 reservoir quality. *American Association of Petroleum Geologists*  
 1371 *Bulletin*, 76, 1137–1152.
- 1372 Macaulay, C. I., Haszeldine, R. S., & Fallick, A. E. (1992). Diagenetic  
 1373 porewaters stratified for at least 35 million years: Magnus Oil Field,  
 1374 North Sea. *American Association of Petroleum Geologists Bulletin*, 76,  
 1375 1625–1634.
- 1376 Marchand, A. M. E., Haszeldine, R. S., Smalley, P. C., Macaulay, C. I., &  
 1377 Fallick, A. E. (2001). Evidence for reduced quartz-cementation rates in  
 1378 oil-filled sandstones. *Geology*, 29, 915–918.
- 1379 Marchand, A. M. E., Smalley, P. C., Haszeldine, R. S., & Fallick, A. E.  
 1380 (2002). Note on the importance of hydrocarbon fill for reservoir quality  
 1381 prediction in sandstones. *American Association of Petroleum Geol-*  
 1382 *ogists Bulletin*, 86, 1561–1571.
- 1383 McAulay, G. E., Burley, S. D., Fallick, A. E., & Kuszniir, N. J. (1994).  
 1384 Paleohydrodynamic fluid flow regimes during diagenesis of the Brent  
 1385 Group in the Hutton-NW Hutton reservoirs: constraints from oxygen  
 1386 isotope studies of authigenic kaolin and reverse flexural modelling.  
 1387 *Clay Minerals*, 29, 609–626.
- 1388 Morton, A. C., Haszeldine, R. S., Giles, M. R., & Brown, S. (1992).  
 1389 *Geology of the Brent Group. Geological Society Special Publications*  
 1390 *61*, Bath: Geological Society.
- 1391 Osborne, M., Haszeldine, R. S., & Fallick, A. E. (1994). Variation in kaolin  
 1392 morphology with growth temperature in isotopically mixed pore-fluids,  
 1393 Brent Group, UK North Sea. *Clay Minerals*, 29, 591–608.
- 1394 Pettijohn, F. J., Potter, P. E., & Seiver, R. (1973). *Sand and sandstone*.  
 1395 Berlin: Springer, p. 617.
- 1396 Richards, P. C. (1992). An introduction to the Brent Group: A literature  
 1397 review. In A. C. Morton, R. S. Haszeldine, M. R. Giles, & S. Brown  
 1398 (Eds.), *Geology of the Brent Group* (pp. 15–26). *Geological Society,*  
 1399 *London, Special Publication*, 61.
- 1400 Taylor, D. J., & Dietvorst, J. P. A. (1991). The Cormorant Field, Blocks  
 211/21a, 211/26a, UK North Sea. In I. L. Abbotts (Ed.), *United*  
 Kingdom oil and gas fields 25 years commemorative volume (pp.  
 73–81). *Geological Society, London, Memoir*, 14.
- Wilkinson, M., Darby, D., Haszeldine, R. S., & Couples, G. D. (1997).  
 Secondary porosity generation during deep burial associated with  
 overpressure leak-off: Fulmar Formation, United Kingdom Central  
 Graben. *American Association of Petroleum Geologists Bulletin*, 81,  
 803–813.
- Wilkinson, M., & Haszeldine, R. S. (2002). Fibrous illite in oilfield  
 sandstones—a nucleation kinetic theory of growth. *Terra Nova*, 14,  
 49–55.
- Wilkinson, M., Haszeldine, R. S., Fallick, A. E., & Osborne, M. J. (2000).  
 Siderite zonation within the Brent Group: microbial influence or aquifer  
 flow? *Clay Minerals*, 35, 107–117.
- Worden, R. H., Smalley, P. C., & Oxtoby, N. H. (1998). Can oil  
 emplacement stop quartz cementation in sandstones? *Petroleum*  
*Geoscience*, 4, 129–138.